

Fig. 3: Hardware and software architectures

(without a polarizer). The IMX250MYR [9] image sensor is a color polarizer filter array (CPFA) image sensor which implements two filter arrays: a color filter array (CFA) and a polarizer filter array (PFA). The polarizers used in this sensor are called wired grid polarizers and they block (by reflection) the polarization parallel to the wire direction while they transmit the polarization normal to the wire direction [11]. A representation of these polarizers and the super pixel array configuration can be seen in Fig. 1.

In every raw image (Fig. 4a) captured with a color polarization image sensor there are 12 different channels: 3 color channels (red, green and blue) and 4 linearly polarized channels ( $0^\circ$ ,  $45^\circ$ ,  $90^\circ$  and  $135^\circ$ ) for each color channel (Fig. 4b). The process of recovering the color information is called CFA demosaicing [12] and the process of recovering the polarizer information is called PFA demosaicing [13].

### III. PROPOSED SYSTEM ARCHITECTURE

#### A. Hardware architecture

The first key component of the hardware architecture (Fig. 3a) is a polarization camera that integrates a Sony CMOS (Complementary Metal-Oxide-Semiconductor) image sensor with a micro-polarizer layer (Fig. 1) together with an FPGA (Field Programmable Gate Array) for the low-level processing and a camera lens. The polarization camera is connected to the computing unit using the USB3 Vision interface which makes use of the GenICam (Generic Interface for Cameras) protocol [14]. For the light source, a Powell lens [15] laser line projector that generates a uniform (non-Gaussian) laser beam is used. The projector is connected to the computing unit using the UART (Universal Asynchronous Receiver-Transmitter) protocol and its laser medium is controlled using TTL (Transistor-to-Transistor Logic). The hardware architecture is built around a computing unit, which main component is an SoC (System on a Chip) that integrates a Central Processing Unit (CPU) and a Graphics Processing Unit (GPU) for tasks that can be highly parallelized (i.e. image processing). The CPU and GPU memory is unified in one memory stack. Additionally, the computing unit implements an Ethernet controller that is used for communicating with the network.

#### Algorithm 1 Polarized laser image pipeline

**Input:** Raw sensor image  $I_{raw}$

**Output:** Position of the laser in image coordinates

- 1: **procedure** POLARLAS( $I_{raw}$ )
- 2:  $(I_0^\circ, I_{45^\circ}, I_{90^\circ}, I_{135^\circ}) \leftarrow PFA_{dem}(I_{raw}) \triangleright$  Pol. dem.
- 3:  $I_{opt} \leftarrow OptPolar(I_0^\circ, I_{45^\circ}, I_{90^\circ}, I_{135^\circ}) \triangleright$  Optimize
- 4:  $I_{opt} \leftarrow CFA_{dem}(I_{opt}) \triangleright$  Color demosaic
- 5:  $I_{opt} \leftarrow ToMono(I_{opt}) \triangleright$  Convert to monochrome
- 6:  $I_{opt} \leftarrow Thresh(I_{opt}) \triangleright$  Apply a threshold
- 7: **for** every column in  $I_{opt}$  **do**  $\triangleright$  Laser line extraction
- 8:  $P_C \leftarrow P_L \triangleright$  Position of the laser in the column
- 9: **return**  $LaserCoordImg \triangleright$  Output is 1 image

#### B. Software architecture

The main application of the software architecture (Fig. 3b) which runs on the computing unit, coordinates the different tasks and is written in C++. Its first task is communicating with the FPGA firmware using the GenICam protocol, in order to start, stop, and configure the image acquisition, in addition to retrieving the actual image data. Inside the application, the camera firmware is accessible via its USB3 Vision interface using the GenICam protocol through the open-source library Aravis [16]. For the image processing part of the application, the OpenCV library, which has GPU acceleration capabilities, is used to compute the pipeline in Algorithm 1. This pipeline can be summed up as acquiring the raw image, performing the PFA demosaicing, performing the CFA demosaicing, creating the optimized image by combining the data of the 4 polarized color images and performing the laser line extraction. Furthermore, the custom application has to control the laser, which is a simple function to turn it on/off or change its intensity. In addition to communicating with the network by means of a middleware solution.

### IV. IMPLEMENTATION

The proposed architecture was implemented as a prototype (Fig. 2). The polarization camera used is a MATRIX VISION mvBlueFOX3-2051pC that integrates a Sony IMX250MYR

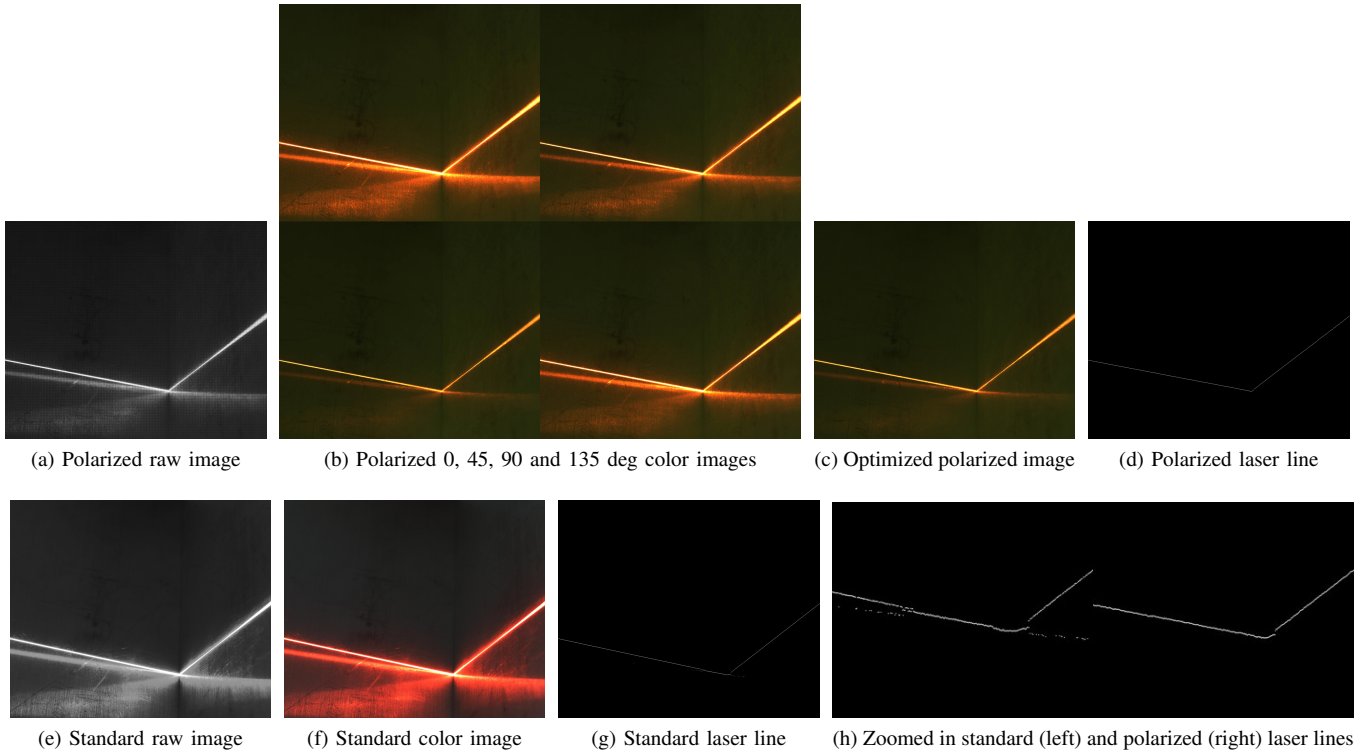


Fig. 4: Comparison between the polarization image sensor and the standard image sensor images

5.07 Megapixels color capable polarization image sensor. For comparison purposes, an OMRON STC-MCS500U3V camera that integrates a Sony IMX264LLR 5.07 Megapixels color capable non-polarized image sensor was used. This standard model of the Sony IMX family was chosen because of its similarity with the IMX250MYR sensor integrated in the polarization camera. Regarding the optics, the same C-Mount FUJINON 1 : 1.4/16 mm CF16 lens was used for both cameras. For the laser projector, a Z-LASER Z25M18S3-F-640-LP45 operating at 640 nm and displaying a single line was chosen. The proposed image pipeline in Algorithm 1 was implemented in a C++ application running in the Linux4Tegra operating system with a Real-Time kernel. Furthermore, it was running on an Nvidia Jetson AGX Xavier that is based on an SoC that integrates an ARM CPU plus an Nvidia GPU.

## V. EXPERIMENTS AND RESULTS

The plates scanned in the experiments were made of aluminium alloy 6082. The alloy was chosen because it is highly reflective [17] and widely used [18]. With regard to the geometry of the experiment, the two aluminium plates were arranged in a corner joint configuration forming a right angle and then firmly clamped, as it can be seen in Fig. 2. The distance from the laser projector to the joint is approximately 30 cm. The results with both sensors are shown in Fig. 4. Note that the optimized polarized image in Fig. 4c displays a substantial reduction in the amount of reflections with respect to the standard color image in Fig. 4f. And, as an outcome,

the shape of the extracted laser line when using the polarized image sensor in Fig. 4d is closer to the real shape of the laser and contains less artifacts when compared to the extracted laser line when using the standard image sensor in Fig. 4g. The benefits of using the polarization image sensor are even more noticeable if the area around the joint is zoomed in as it can be seen in Fig. 4h, where the standard image sensor struggles to detect the real shape of the laser in certain parts of the profile, generating artifacts in the image, in addition to deforming the shape of the corner. Meanwhile, the polarized image sensor manages to detect most of the laser profile correctly, with only 4 pixels of a tiny area of the profile not detected properly.

## VI. CONCLUSIONS

As the results show, under similar circumstances (same image sensor family, laser projector, lens, and hardware and software platforms), the proposed novel laser scanner based on a polarization image sensor can detect the shape of a laser profile in a more precise way than a standard image sensor can when scanning very reflective aluminium alloys. Although there are some limitations in areas containing great amounts of specular reflections. We believe that these results are especially interesting for robotics applications like industrial robotic welding, where measuring the accurate position of the corners or joints of the scanned metallic plates is essential.

## ACKNOWLEDGMENT

The presented work is funded by the Research Council of Norway under MAROFF Project Number 295138.

## REFERENCES

- [1] M. Ribo and M. Brandner, "State of the art on vision-based structured light systems for 3D measurements," in *International Workshop on Robotic Sensors: Robotic and Sensor Environments, 2005*. IEEE, 2005, pp. 2–6.
- [2] M. A. Isa and I. Lazoglu, "Design and analysis of a 3D laser scanner," *Measurement*, vol. 111, pp. 122–133, 2017.
- [3] A. Donges and R. Noll, *Laser measurement technology*. Springer, 2016.
- [4] J. L. Vilaça, J. C. Fonseca, and A. M. Pinho, "Non-contact 3D acquisition system based on stereo vision and laser triangulation," *Machine Vision and Applications*, vol. 21, no. 3, pp. 341–350, 2010.
- [5] J. Balzer and S. Werling, "Principles of shape from specular reflection," *Measurement*, vol. 43, no. 10, pp. 1305–1317, 2010.
- [6] Z. Song, H. Jiang, H. Lin, and S. Tang, "A high dynamic range structured light means for the 3D measurement of specular surface," *Optics and Lasers in Engineering*, vol. 95, pp. 8–16, 2017.
- [7] J. Clark, E. Trucco, and H.-F. Cheung, "Improving laser triangulation sensors using polarization," in *Proceedings of IEEE International Conference on Computer Vision*. IEEE, 1995, pp. 981–986.
- [8] J. Clark, E. Trucco, and L. B. Wolff, "Using light polarization in laser scanning," *Image and Vision Computing*, vol. 15, no. 2, pp. 107–117, 1997.
- [9] "Sony semiconductor solutions corporation. polarization image sensor with four-directional on-chip polarizer and global shutter function." (Date last accessed 16-June-2021). [Online]. Available: <https://www.sony-semicon.co.jp/e/products/IS/industry/product/polarization.html>
- [10] R. A. Chipman, W. S. T. Lam, and G. Young, *Polarized light and optical systems*, 1st ed. CRC Press, 2018, pp. 63–85.
- [11] P. Yeh, "A new optical model for wire grid polarizers," *Optics Communications*, vol. 26, no. 3, pp. 289–292, 1978.
- [12] D. Alleysson, S. Susstrunk, and J. Hérault, "Linear demosaicing inspired by the human visual system," *IEEE Transactions on Image Processing*, vol. 14, no. 4, pp. 439–449, 2005.
- [13] S. Mihoubi, P.-J. Lapray, and L. Bigué, "Survey of demosaicking methods for polarization filter array images," *Sensors*, vol. 18, no. 11, p. 3688, 2018.
- [14] "Genicam. the generic interface for cameras standard," (Date last accessed 16-June-2021). [Online]. Available: <https://www.emva.org/standards-technology/genicam/>
- [15] A. Bewsher, I. Powell, and W. Boland, "Design of single-element laser-beam shape projectors," *Applied optics*, vol. 35, no. 10, pp. 1654–1658, 1996.
- [16] "Aravis. a vision library for genicam based cameras," (Date last accessed 16-June-2021). [Online]. Available: <https://github.com/AravisProject/aravis>
- [17] O. O. Oladimeji and E. Taban, "Trend and innovations in laser beam welding of wrought aluminum alloys," *Welding in the World*, vol. 60, no. 3, pp. 415–457, 2016.
- [18] J. R. Kissell and R. L. Ferry, *Aluminum structures: a guide to their specifications and design*. John Wiley & Sons, 2002.